

The Calibration and Monitoring System for the PHENIX Lead-Scintillator Electromagnetic Calorimeter¹

G.David, E.Kistenev, S.Stoll, S.White, C.Woody
Brookhaven National Laboratory, Upton, New York

A.Bazilevsky, S.Belikov, S.Chernichenkov, A.Denisov, Yu. Gilitzky, V.Kochetkov, Y.Melnikov, V.Onuchin,
A.Semenov, V.Shelikhov, A.Soldatov

Institute for High Energy Physics, Protvino, Russia

Abstract

The calibration and monitoring system for the PHENIX lead-scintillator electromagnetic calorimeter is described along with the experience obtained in using this system to calibrate calorimeter modules with cosmic rays. The system is based on a UV laser which delivers light to each module through a series of optical fibers and splitters that is monitored at various points using silicon and vacuum photodiodes. Results are given from a prototype system based on a nitrogen laser which was used to monitor the stability of several modules, as well as to set the gains of the phototubes and establish the energy calibration of all calorimeter modules before installation into the final detector. A description of the final system to be used in PHENIX, based on a high power YAG laser, is also given.

I. INTRODUCTION

The lead-scintillator electromagnetic calorimeter for the PHENIX experiment is a shashlik type detector [1] consisting of 15552 individual towers and covers an area of approximately 48 m². The calorimeter will be used to measure electron and photon production in relativistic heavy ion collisions at RHIC, and will be an integral part of the particle identification and trigger system for PHENIX. In addition, the calorimeter will be used to measure high p_T photon production and other electromagnetic processes in high energy polarized proton collisions as part of the spin physics program at RHIC.

The calorimeter has a nominal energy resolution of $8\%/\sqrt{E}(\text{GeV})$ and a timing resolution of ≤ 100 ps for electromagnetic showers [2]. Given the size of the calorimeter and the large number of channels, the calibration, stabilization and gain monitoring of such a large system is a formidable task. As a result, an extensive precision calibration and monitoring system has been developed to achieve a predetermined absolute energy calibration of less than 5% for day one operation at RHIC, and to maintain an overall long term gain stability of less than 1%. The overall design of the system will be described, and results will be presented from various tests and module calibrations using cosmic rays. Other similar types of systems are described in refs.[3][4].

¹This work was supported under DOE Contract DE-AC02-76CH00016

II. SYSTEM DESIGN

The calibration and monitoring system is based on a UV laser which supplies light to the calorimeter through a system of optical splitters and fibers. The calorimeter is arranged into six sectors, each consisting of a 3×6 array of 18 supermodules. Each supermodule consists of a 6×6 array of individual modules, each containing four readout towers with four phototubes. Light is injected into each module through a "leaky fiber" which excites the plastic scintillator stack with a distribution in depth that simulates an electromagnetic shower. The intensity of the light at each supermodule is monitored with a PIN diode that is used for normalization. The light intensity is also monitored with additional PIN diodes at each intermediate splitter, as well as directly from the laser at the initial beam splitter using a biplanar phototube.

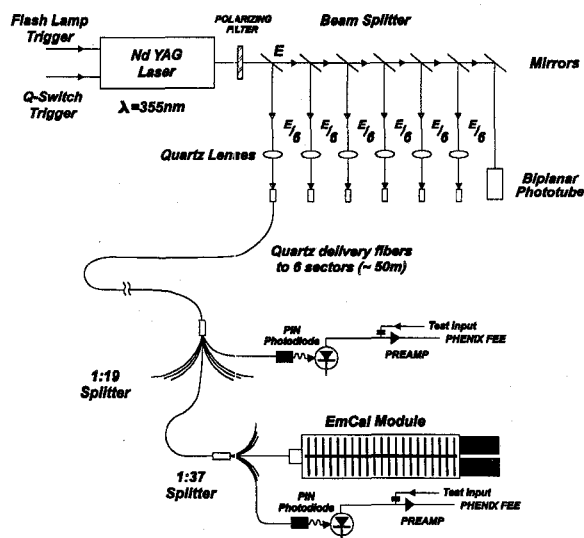


Fig. 1 Laser calibration, monitoring and light distribution system

A. Laser and Primary Beam Splitter

The overall layout of the system is shown in Fig. 1. A UV laser is used as the primary light source which supplies light to each of the six sectors. For the initial precalibration of the final calorimeter modules using cosmic rays, a pulsed nitrogen laser (Laser Science VSL-337ND) was used which had an output power of 250 μW and produced an output pulse approximately 3 ns wide at a wavelength of 337 nm. For the final system, a

high power YAG laser (Continuum Surelite II-10) will be used in order to provide sufficient energy to all of the 3888 individual calorimeter modules after several levels of splitting in the light distribution system. The laser is equipped with two harmonic generators which are used to shift the wavelength of the primary beam of the YAG laser from 1064 nm to the third harmonic at 355 nm (a second harmonic beam at 532 nm is also produced). The maximum output power at 355 nm is more than 2 W (200 mJ per pulse at 10 Hz) with a pulse width of ~ 6 ns, although usually only a small fraction (typically $\leq 10\%$) is used to deliver light to the calibration system. The beam intensity is controlled by a set of fixed attenuators plus a remotely controlled variable attenuator. The variable attenuator consists of a half wave plate mounted on a rotatable stage which can change the polarization angle of the initially horizontally polarized light produced by the laser. The polarization angle is rotated to produce varying amounts of horizontally and vertically polarized components, and the beam is then passed through a birefringent splitter cube which spatially separates the two components. The horizontal component is passed through to the primary beam splitter, while the vertical component is passed onto a beam dump. A precision remotely controlled rotation stage controls the angle of the half wave plate, and hence the amount of horizontally polarized light which is delivered to the primary beam splitter.

Light from the laser is initially split into six equal intensity beams using a set of partially reflecting mirrors. The beam from each mirror passes through a quartz lens and is focused to a point just in front of a quartz fiber. These are long delivery fibers used to transport the light over a distance of approximately 50 m to each sector of the calorimeter, and they must therefore have a long attenuation length for UV light. They will be 600 μm silica-core/silica-cladding high OH^- fibers (3M Specialty Fiber FG-600-UAT) which have numerical aperture of 0.16 and an attenuation length of 60 dB/km at 355 nm. In addition, they are designed for high power applications (up to 5 GW/cm^2) in order to handle the extremely high instantaneous power of the focused laser beam. It is nevertheless important to provide the proper "launch conditions" at the injection point of the fiber in order to avoid damage the fiber end. The lenses have a focal length of 6.5 cm and the beam diameter is approximately 6 mm. The fiber is placed at a distance of 5 mm from the focal point of the lens, which produces a beam spot of $\sim 460 \mu\text{m}$ at the fiber face. It is important that this spot size be kept small (≤ 0.8 times the fiber diameter) in order to prevent light from entering the cladding which can damage the fiber. In addition, the injection angle (θ) must not be too large or too small compared to the numerical aperture of the fiber (typically $0.3 \text{ NA} \leq \theta \leq 0.8 \text{ NA}$) or possible fiber damage can occur.

B. Optical Splitters

A system of optical splitters is used to distribute the light to each of the individual calorimeter modules. This is accomplished using two levels of optical splitting. The first splitter is located at the end of the long delivery fibers (one for each calorimeter sector), and divides the light into 21 output fibers. Eighteen of the output fibers are used to deliver light to the eighteen supermodules within one sector, one is used

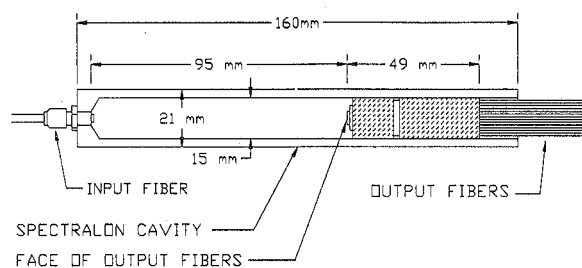


Fig. 2 First level optical splitter (1:21)

for monitoring, as described below, and two are spares. The splitter, shown in Fig. 2, is arranged such that the input fiber projects a spot of light onto a bundle of output fibers located some distance away. The fibers are mounted inside a high reflecting cavity made of Spectralon² which serves to collect the light leaving the delivery fiber that is not directly projected onto the output fiber bundle. This feature greatly improves the efficiency and uniformity of the output fibers. Figure 3 shows the dependence of the efficiency of the output fibers as a function of the separation distance from the input fiber to the output fiber bundle. The efficiency is defined as the ratio of the light intensity of an individual output fiber to the total light delivered to the input fiber. The uniformity is measured in terms of the standard deviation of the output fiber intensities, as well as the "max/min ratio", which gives the ratio of the highest intensity to lowest intensity output fibers. The uniformity is strongly dependent on the cavity spacing for short distances, but is limited by other factors pertaining to the fibers, such as end preparation and polish, for larger distances. In the final design, a cavity spacing of approximately 70 mm will be used, which gives an individual fiber efficiency of 2.8×10^{-3} , a uniformity with a σ/mean of 5.3%, and a max/min ratio of 1.25.

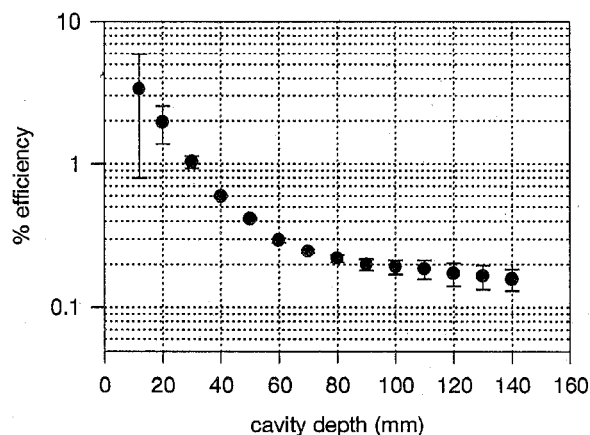


Fig. 3 Efficiency of 1:21 splitter as a function of cavity depth

Each of the 18 outputs of the first level splitter is connected via a 5 m long 1 mm dia. UV transmitting plastic fiber (Hoechst-Celanese FP200) to a second level splitter inside each of the supermodules. The design of the second splitter

²Spectralon is a product of Labsphere Corp., North Sutton, NH

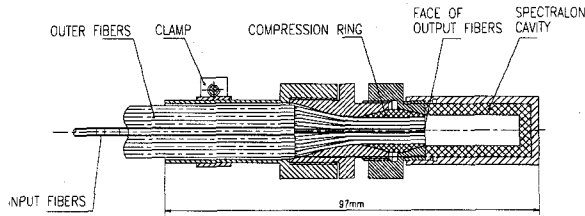


Fig. 4 Second level optical splitter (1:38)

is similar to the first except that the input fiber is included within the bundle of output fibers and projects light onto the back surface of the Spectralon cavity. As shown in Fig. 4, this allows for a more compact design in which the splitter acts as a simple integrating sphere giving good output fiber uniformity. The output consists of a total of 38 output fibers, 36 of which go to each of the 36 individual calorimeter modules within each supermodule, one which goes to a PIN diode reference located inside the supermodule, and another which goes to an external PIN diode located outside the supermodule. The performance of the second level splitter is similar to the first level splitter. The individual output fiber efficiency is of order 2.2×10^{-3} , and the uniformity can be characterized with a σ/mean of 7.3% and a max/min ratio of 1.32.

C. Calorimeter modules

The output fibers of the second level splitter are connected via short (~ 60 cm) 1 mm dia. plastic fibers to each calorimeter module within the supermodule. The light is injected into a so-called "leaky fiber" which allows the light to leak out of the fiber in such a way as to simulate an electromagnetic shower penetrating along the depth of the module. This is accomplished by scribing a spiral scratch along a 38 cm long \times 2 mm dia. plastic fiber which is inserted into a hole in the center of the module. Light escapes from the fiber according to a prescribed pattern along its length which excites the plastic scintillator tiles within the calorimeter stack. Figure 5 shows a cutaway view of a calorimeter module showing the the location of the leaky fiber along with the lead-scintillator stack and readout wavelength shifting fibers.

The scribe pattern was determined experimentally by measuring the light output as a function of position along the fiber with a small piece of scintillator surrounding the fiber. The pattern was tuned to give a depth profile which resembled an electromagnetic shower with an energy of approximately 1 GeV. Figure 6 shows the depth profile for a group of scribed fibers compared to a 1 GeV shower simulated using GEANT. More than 4000 fibers were scribed using a computer controlled scribing machine which consisted of fine point cutting tool mounted on a long screw thread driven by a programmable stepping motor. The depth profile was very sensitive to the depth of the scribe made by the cutting tool and had to be controlled very carefully to avoid large variations in the resulting pattern. However, the overall efficiency of the leaky fiber to deliver light to the module was less sensitive to the actual pattern and was measured to be $\geq 90\%$. The overall efficiency for converting UV light injected into the module to visible light produced at the output bundle of wavelength

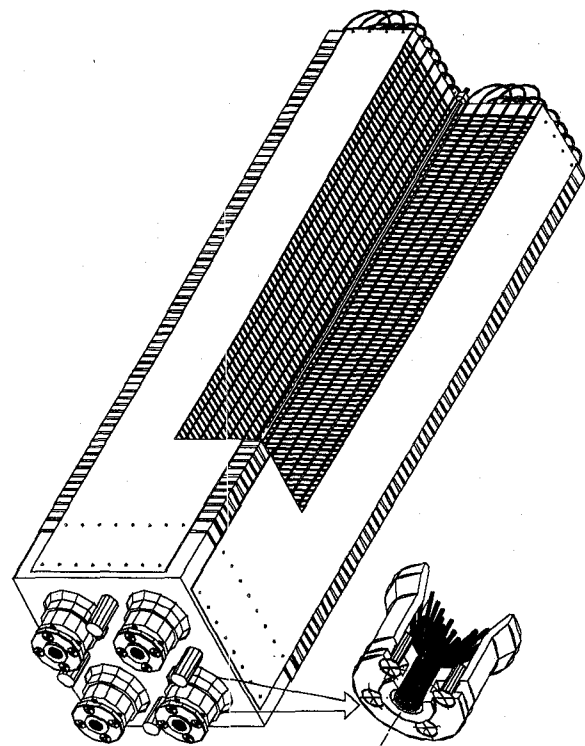


Fig. 5 Interior view of calorimeter module showing stack of scintillator and lead plates, wavelength shifting fiber readout, and leaky fiber inserted in central hole

shifting fibers was $\sim 7.6 \times 10^{-4}$. This efficiency includes the leaky fiber efficiency, the conversion efficiency from UV light to blue scintillation light inside the scintillator, and the conversion efficiency of the scintillation light into green light in the wavelength shifting fibers.

The total efficiency for the conversion of UV light from the laser to photoelectrons in the readout phototubes is extremely small given the numerous inefficiencies involved. Table I gives a list of the contributions to the overall efficiency from the various parts of the light distribution system. The overall efficiency to convert the primary light from the laser to

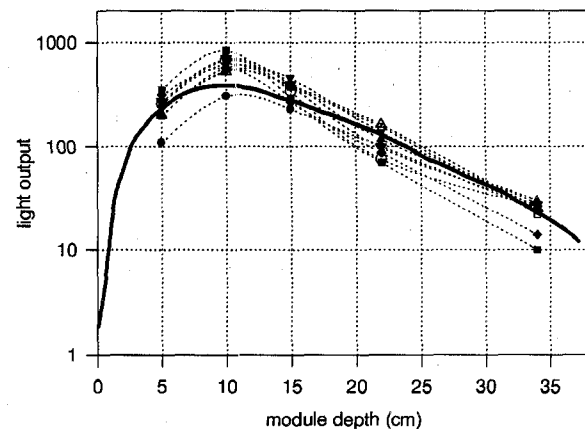


Fig. 6 Light output profile as a function of depth for leaky fibers. Solid curve shows 1 GeV electromagnetic shower profile from GEANT simulation

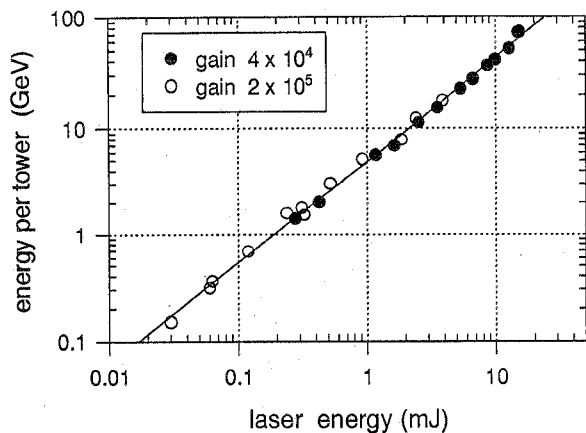


Fig. 7 Equivalent energy per module versus beam energy for YAG laser.

photoelectrons in an individual module is of order 4.2×10^{-12} , which determines the power requirements of the laser. This has been measured with the YAG laser for the final PHENIX system and is shown in Fig. 7. Given that the calorimeter has an intrinsic light output of ~ 1500 photoelectrons per GeV, this leads to an energy requirement of ~ 0.2 mJ per pulse from the YAG laser to deliver 1 GeV of equivalent energy to each module at a phototube gain setting appropriate for heavy ion running at RHIC ($\sim 2 \times 10^5$). Linearity studies and calibration of the calorimeter for high energy polarized proton running at RHIC (which would be done at a lower gain setting of $\sim 4 \times 10^4$) can require up to 80 GeV per module, or 16 mJ per pulse from the laser.

Table 1
Light Distribution System Efficiencies

Component	Efficiency
Initial beam split	.17
Injection into fiber	1.0
Delivery fiber (50 m)	0.5
First level splitter (1:21)	2.8×10^{-3}
Second level splitter (1:38)	2.2×10^{-3}
Module conversion efficiency	7.6×10^{-4}
Efficiency of connections and other losses	.07
Photomultiplier Quantum Efficiency losses	0.15
Total efficiency	4.2×10^{-12}

III. MONITORING PHOTODIODES

Since the energy of the laser varies from pulse to pulse with an rms variation of $\sim 4\%$, and the average energy can change over periods of hours by more than 10%, it is necessary to measure the light output of the laser pulse by pulse with a stable reference device and compare this to the light output measured in each module. The light intensity is measured at various places throughout the light distribution system using a system of silicon PIN photodiodes, as well as at the primary beam splitter using a biplanar photodiode. The biplanar phototube (Hamamatsu R1328U-02) is a highly linear vacuum photodiode with a high current photocathode which is capable

of measuring direct light from the laser. As shown in Figure 1, it is located at the end of the set of six primary beam splitter mirrors and sees a small fraction of the light ($\sim 1\%$) which passes through the last mirror. It is therefore the primary reference monitor of the beam intensity.

A collection of PIN photodiodes (Hamamatsu S-1223-01) are used to monitor the light intensity after each level of splitting. One diode is used to measure the output of each of the 1:21 splitters for each sector. This diode will be located on the interior wall of the sector along with other photodiodes used to monitor the light delivered to each supermodule. Each supermodule contains a 1:38 splitter which delivers light using 36 output fibers to each module within that supermodule, and two outputs used for monitoring. One output goes to an internal PIN photodiode located underneath the front cover of the supermodule and is used as the primary reference for that supermodule. The second monitor output is connected to a ~ 5 m long 1 mm dia. plastic fiber which carries the light to an external photodiode located on the interior wall of the sector. This diode is used as a secondary reference for the supermodule, and compared to the primary internal photodiode reference for consistency and redundancy. It also allows access to the secondary reference diode after installation, since the primary reference diode is inaccessible once the calorimeter is installed at RHIC.

The internal PIN diodes are read out using a high speed voltage amplifier (Elantec 2075) which delivers a signal along a 100 ohm twisted pair cable to the PHENIX front end readout electronics. Each diode readout circuit also contains a stable current-mirror source which is switched by an external ECL trigger to deliver a calibration pulse to the voltage amplifier. This calibration pulse is used to monitor the stability of the amplifier and to conveniently test the rest of the readout chain. The readout circuit for the external photodiode is currently still being designed, but will be similar to the one used for the internal photodiodes.

IV. ENERGY CALIBRATION AND GAIN MONITORING

The laser calibration and gain monitoring system has been used extensively to study several prototype calorimeter modules in a number of beam tests at the Brookhaven AGS, and is presently being used to establish the initial phototube gain settings and operating conditions for each production calorimeter module as it is prepared for initial operation RHIC. For these applications, a prototype version of the system was used which contains a nitrogen laser. The final system based on the YAG laser is nearly complete and is presently being tested.

Each calorimeter supermodule which will be installed in PHENIX undergoes a precalibration procedure using cosmic rays to determine the initial gain settings and operating conditions. Initially, each supermodule is equipped with the same set of 144 phototubes which are used to measure the light output from each tower using cosmic ray muons which pass through the modules transversely. This is done at a fixed gain setting for each tube, and the same setting

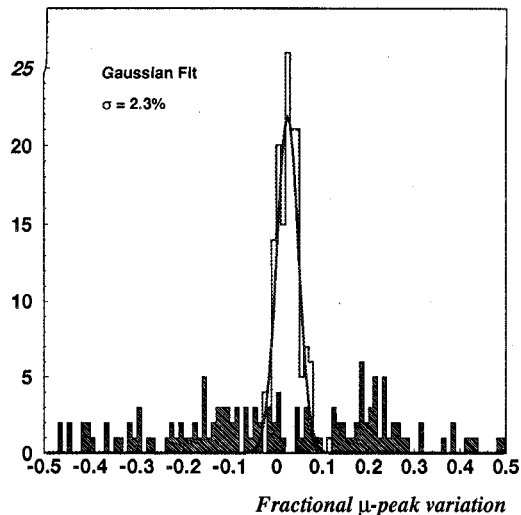


Fig. 8 Deviation from initial muon calibration of all channels of one supermodule after installation of final phototubes. Shaded area is without renormalization using laser calibration and open histogram is with renormalization.

is used for each supermodule. A spectrum of cosmic ray muons corresponding to an energy deposit of approximately 38 MeV is accumulated for each tower, while at the same time a spectrum of laser events is collected for the each tower and for the internal reference photodiode. The ratio of the signal from the module to the signal from the photodiode is independent of the intensity of the light from the laser and serves as the reference to re-establish the same phototube response (given by the product of gain times quantum efficiency) for the final set of phototubes which are installed in the supermodule. The final tubes are selected from a set of pre-measured tubes and are installed in the supermodule in three groups of 48 tubes with similar gains. This grouping is due to the fact that the high voltage is supplied to the calorimeter in such a way that all 48 tubes within a given group operate at the same high voltage. Therefore, when the final tubes are installed, there is a large dispersion in the actual response of each tower to the original muon calibration. However, as shown in Fig. 8, when the response is renormalized to the original reference response using the laser, the dispersion is reduced to only 2.3%. This residual dispersion is due mainly to the variation in the quantum efficiencies of the phototubes, but is more than a factor of two better than the design goal of 5% in predetermining the initial energy calibration of the calorimeter for RHIC operation.

In order to determine the ability of the calibration system to monitor and correct for phototube gain variations, a test was done to measure the change in muon response over time of a supermodule with a given set of phototubes at a fixed high voltage. The module was calibrated using cosmic ray muons with the standard set of phototubes used for precalibrating all supermodules, and the tubes were left on at their nominal operating voltage. Periodic measurements were then made of the muon calibration and compared to the initial value.

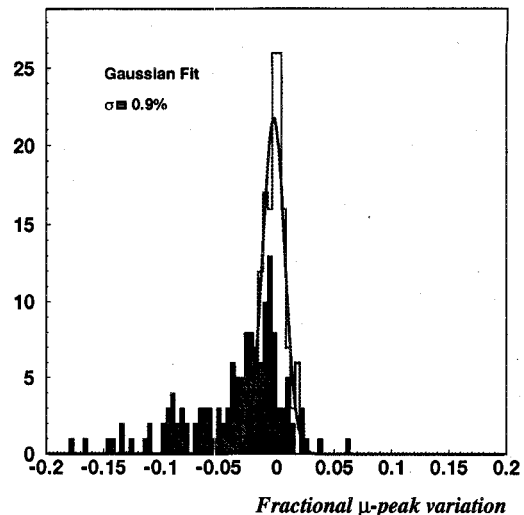


Fig. 9 Deviation from initial muon calibration of all channels of one supermodule with no change in phototubes or phototube high voltage after one week. Shaded area is without renormalization using laser calibration and open histogram is with renormalization.

Figure 9 shows the deviation of all phototubes within the supermodule from their initial calibration over a period of one week with and without renormalization using the laser calibration system. After renormalization, the gain drift variation is reduced to 0.9%. Although the long term stability has only been measured for a limited number of supermodules, it is expected that all supermodules will perform in a similar manner, and that a long term stability limit of $\sim 1\%$ can be achieved for the entire system.

V. CONCLUSIONS

A precision calibration and monitoring system has been designed for the PHENIX lead-scintillator electromagnetic calorimeter which is being used in conjunction with cosmic ray muons to predetermine the initial energy calibration of the calorimeter to better than 5% and to monitor gain drifts to $\sim 1\%$. The system has been used to precalibrate more than half the total number of modules which will be installed at RHIC and has performed more than a factor of two better than the design goal. It has also been shown that the system can monitor gain drifts in the phototubes to the required precision, and it is therefore expected that the final system will meet the necessary performance requirements for the PHENIX calorimeter. The final system should be completed by the middle of 1998.

VI. REFERENCES

- [1] PHENIX Conceptual Design Report, BNL 48922, Jan. 29, 1993.
- [2] G.David et al., "Performance of the PHENIX EM Calorimeter", *IEEE Trans. Nucl. Sci.* NS-43 (1996) 1491-1495.
- [3] OPAL Collaboration, K.Ahmet et al., *Nucl. Inst. Meth.* A305 (1991) 275.
- [4] CDF Collaboration, S.Bertolucci et al., *Nucl. Inst. Meth.* A267 (1988) 301.